J Supercond Nov Magn (2008) 21: 467–472
DOI 10.1007/s10948-008-0386-0

ORIGINAL PAPER

3D-Modeling Numerical Solutions of Electromagnetic Behavior of HTSC Bulk above Permanent Magnetic Guideway

Yiyun Lu · Jiasu Wang · Suyu Wang · Jun Zheng

Received: 3 October 2008 / Accepted: 22 October 2008 / Published online: 5 November 2008

Abstract This paper presents a 3D-modeling numerical method using finite element method (FEM) to simulate the electromagnetic behavior of high-temperature superconductors (HTSC). The models are formulated by the magnetic field vector method (H-method). The resolving code was written by FROTRAN language. The electromagnetic properties of HTSC are described though Kim critical-state model. The magnetic fields and current distribution in the bulk HTSC in the applied non-uniform external magnetic fields generated by the permanent magnetic guideway (PMG) are obtained using the proposed method. The magnetic levitation forces by the interaction between the bulk HTSC and the PMG are calculated. In order to validate the method, measurement of the vertical force between a bulk YBaCuO(YBCO) and a PMG is obtained. The measurement and simulation results show good matching. This method could be used in the HTSC magnetic levitation transportation system optimization design.

Keywords Permanent magnetic guideway · 3D-model · High-temperature superconductors · Finite element method

PACS 85.25.-j

1 Introduction

After the discovery of intrinsic stable levitation (or suspension) of bulk high-T_c superconductors (HTSC) above (or below) permanent magnet, some potential applications using bulk HTSC, bearing, flywheel and Maglev transportation, are expected [1–4]. It is necessary to be able to well predict the electromagnetic behavior of those devices in order to optimize their performance. Because the electromagnetic properties of HTSC are highly nonlinear, it is difficult to simulate their behavior. These nonlinear characteristics are material anisotropism and E-J constitutive law nonlinearity. For grain boundary of bulk YBCO, critical current density along a-b plane is about three times that along c-axial in the bulk YBCO interior. These are the anisotropic properties of HTSC materials. For E-J constitutive law, it is different with normal conductors. Lots of proposed models have been developed to describe that E-J relation. The Bean critical-state model is the most popular one. The Bean model assumes that there is only nonzero electrical field existing in the interior of HTSC where superconducting current density can be generated, and the inducing current density equals to its critical value J_c which is independent of magnitude of the electric field. The Kim critical model assumes that J_c is dependent on local magnetic field. The flux flow and creep model could explain the phenomena of the magnetic force time dependence of high-T_c superconductors. This is due to the motion of fluxiods which induce the electromotive force. The critical current density J_c not only depends on material and temperature but also on local current density and magnetic field. Usually a highly non-linear E-J constitutive law is used to describe this behavior. The most effective way to deal with this problem is to use some iterative methods. They consume more computing time.

During the past years, several numerical and analytical methods have been proposed to carry out this work. For 2D-models, limited to relatively simple geometries under homogeneous or axially symmetric external fields, several analytical methods have been developed [5–7]. Two-dimensional semi-infinite domains and axially symmetric

Y. Lu (✉) · J. Wang · S. Wang · J. Zheng
Applied Superconductivity Laboratory, Southwest Jiaotong University, P.O. Box 152, Chengdu, Sichuan 610031, People's Republic of China
e-mail: luyiyun6666@vip.sohu.com

domains are considered to carry out numerical methods, such as A-V formulation [8–10], H-formulation [11] and T-formulation [12]. For the 3D-models, because of difficulty of dealing with the high nonlinear properties and limited computer ability, seldom a report has been seen. R. Pecher developed a 3D-modeling mathematical method by applying the edge element based Galerkin technique [13]. By stacking multiple 2D-layers on top of each other, some quasi-3D geometries could be achieved [14]. This method ignores the current density flowing along c-axis by assuming the axial-symmetric geometries and external fields.

In this paper, a 3D modeling numerical method is being introduced by finite element method (FEM) to simulate the electromagnetic behavior of HTSC. Expression $E_{sc} = E_{c0} \cdot (J_{sc}/J_c(H_{sc}))^n$ is used to describe E-J relationship of HTSC. Two virtual bulk HTSC are proposed for solving the material anisotropism problem of HTSC. One simple iterative method is used to solve the E-J nonlinear characteristic of HTSC. Forward finite difference is used for solving time variety problem.

The superconducting levitation system composed of one bulk YBCO and PMG is successfully investigated using the proposed method. This levitation system is the prototype system of the first man-loading HTSC Maglev system [4]. The simulation results show that HTSC of mix-state resist magnetic fluxon variation and then the inducing currents result in electromagnetic forces. The resolving code is successfully developed with FORTRAN language.

2 Numerical Scheme

This section consists of three parts. The first part shows the basic equations used to describe the 3D superconducting model, shown in Fig. 1. Then in the second part we simply introduce the boundary conditions. The finite method using the above mathematical models is introduced in part three. In the last part we introduce the resolved code programming procedures.

2.1 Basic Equations

We consider a 3D space with a bulk HTSC subdomain Ω1 and non-superconducting subdomain Ω2 shown as Fig. 1. The dielectric subdomain Ω2 here is air. During the experiment, the YBCO bulk is immersing into liquid nitrogen. In order to simplify the simulating method, we just take it as an air. According to the Maxwell Ampere's Law and Faraday's Law:

$$\nabla \times H = J + \frac{\partial D}{\partial t}, \tag{1}$$

$$\nabla \times E = -\frac{\partial B}{\partial t}. \tag{2}$$

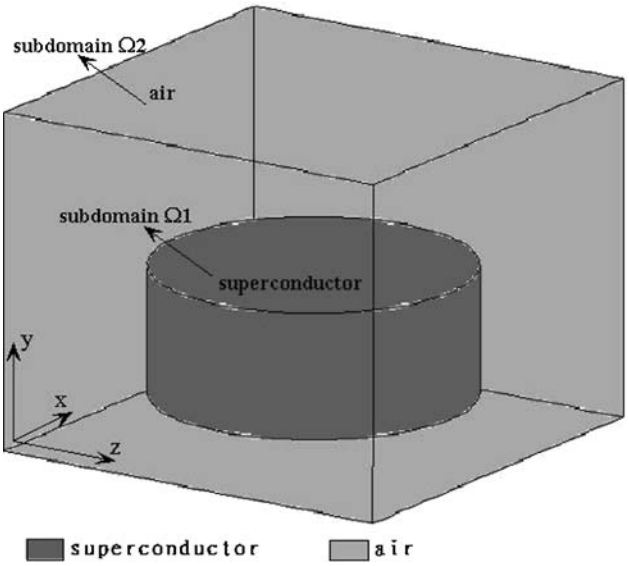

Fig. 1 Diagram of 3D superconducting model

The B-H constitutive law:

$$B = \mu H, \tag{3}$$

where ∇ is the gradient operator; μ is the magnetic permeability. For (1), because of the quasi-approximation problems, we assume no displacement currents are considered: $\partial D/\partial t = 0$.

To the high-T_c superconductors, we use (4) to describe their electrical behavior:

$$E_{sc} = E_{c0}\left(\frac{J_{sc}}{J_c(H_{sc})}\right)^n. \tag{4}$$

Here E_{c0} is material and temperature dependent constants. E_{sc}, J_{sc} and H_{sc} are the electrical field, current density and magnetic field of the high-T_c superconductor, respectively. J_c is the critical current density. In this paper, we choose the value $n = 20$. In this case of the HTS, the effective conductivity depends on the current density and can be represented by the nonlinear power law relation equal to (4):

$$\frac{1}{\sigma_{sc}} = \frac{E_{sc}}{J_{sc}} = \frac{E_{c0}}{J_c}\left(\frac{J_{sc}}{J_c}\right)^n \tag{5}$$

σ_{sc} is the effective conductivity of the superconductor.

The critical current density J_c can be a function of magnetic field as the Kim model:

$$J_c(H_{sc}) = \frac{J_{c0}}{1 + H_{sc}/H_{c0}}. \tag{6}$$

Here J_{c0} and H_{c0} are the material and temperature dependent constants.

For 3D modeling of anisotropic HTSC nonlinear materials problem, the critical current density J_c along c-axis

is considered to be one third of the critical current density flowing along a-b plane in the bulk YBCO interior. We assume that the resistance of the currents flowing along c-axis are three times that along a-b plane. Considering it, (5) can written by:

$$E_{sc} = \begin{bmatrix} E_{sc\_x} \\ E_{sc\_y} \\ E_{sc\_z} \end{bmatrix} = \frac{1}{\sigma_{sc}} \begin{bmatrix} J_{sc\_x} \\ 3 * J_{sc\_y} \\ J_{sc\_z} \end{bmatrix}. \tag{7}$$

Substituting (2) and (3) into (7) we can get the equation:

$$\frac{1}{\sigma_{sc}} \nabla \times \left\{ \begin{bmatrix} J_{sc\_x} \\ J_{sc\_y} \\ J_{sc\_z} \end{bmatrix} + \begin{bmatrix} 0 * J_{sc\_x} \\ 2 * J_{sc\_y} \\ 0 * J_{sc\_z} \end{bmatrix} \right\} = -\mu \frac{\partial}{\partial t} H. \tag{8}$$

Here the bulk HTSC is mathematically composed by two parts, one a homogeneous HTSC and the other only the c-axis oriental conductivity which is not equal to zero. Take account of all the regions, substitute (1) into (8) and consider $J_{sc\_y} = \partial H_x/\partial z - \partial H_z/\partial x$, then (7) can be rewritten as:

$$\mu \frac{\partial}{\partial t} H + \nabla \times \frac{1}{\sigma} \nabla \times H + \frac{\lambda}{\sigma} \nabla \times Q = 0. \tag{9}$$

Here $\sigma = \sigma_{\text{air}}$, $\lambda = 0$ for $\Omega 1$ and $\sigma = \sigma_{sc}$, $\lambda = 1$ for $\Omega 2$ (see Fig. 1), and define Q as:

$$Q = \begin{bmatrix} 0 & 2 * (\frac{\partial H_x}{\partial z} - \frac{\partial H_z}{\partial x}) & 0 \end{bmatrix}^T.$$

Generally, formulation (9) is a time-varying electro-magnetic partial deferential equation derived from Faraday's law, Ampere's law, E-J constitutive power law. The displacement current is ignored in Ampere's law. The components H_x, H_y, H_z of vector magnetic field H are state variables.

2.2 Boundary Conditions

A stable resolution of partial differential equation needs some suitable boundary conditions. For governing equation (9), Dirichlet and Neumann boundary conditions are used to describe the electromagnetic situations. Consider the situation of a bulk HTSC in a non-uniform external magnetic field. The boundary condition between the bulk HTSC and dielectric subdomain $\Omega 1$ region is continuity:

$$\mu_1 H_{1n} = \mu_2 H_{2n}. \tag{10}$$

The outer boundary of subdomain $\Omega 2$ is the dynamic boundary. Here we use a time dependence function to describe:

$$H_{\Omega 2}(r, t) = f_{\Omega 2}(r, t) \tag{11}$$

where the function of $f_{\Omega 2}(r, t)$ describes how the non-uniform external magnetic field changes with time at the outer boundary of subdomain $\Omega 2$. In this paper, the applied magnetic field is generated by the PMG. In our program we used equivalent current model and analysis method to simulate the magnetic field of the PMG.

2.3 Numerical Methods

In this paper, we use the FEM and finite differences to establish the numerical code to solve the nonlinear problem of the bulk YBCO electromagnetic behavior in applied non-uniform external magnetic field. Time differences are used to discretize the time derivative item equal to (9) in time space. FEM is used to discretize the regions described in Fig. 1. The iteration approach is chosen to solve the nonlinearity:

$$\mu \frac{\partial H_n^{i+1}}{\partial t} + \nabla \times \frac{1}{\sigma_n^i} \nabla \times H_n^{i+1} + \frac{\lambda}{\sigma_n^i} \nabla \times Q_n^{i+1} = 0. \tag{12}$$

With the outer boundary conduction (11), the initial conditions are taken into account by:

$$t = 0: \quad H = H_0, \quad H_{\Omega 2}(r, t = 0) = f_{\Omega 2}(r, t = 0). \tag{13}$$

The superscript i $(i = 1, 2, \ldots)$ indicates the number of iteration step. The subscript n indicates the number of time derivation step. Here we use forward-differences method for the time variable problem. When calculation region is in the superconductor, the effective conductivity $\sigma = \sigma_{sc}$. Equation (12) can be rewritten by:

$$\mu H_n^{i+1} + dt \nabla \times \frac{1}{\sigma_n^i} \nabla \times H_n^{i+1} + \frac{\lambda\, dt}{\sigma_n^i} \nabla \times Q_n^{i+1} = \mu H_{n-1} \tag{14}$$

where H_{n-1} is the stable solution of the nth step of time derivation and dt is the step size of each time derivative step.

For FEM, tetrahedron element is chosen for the discretization of the regions. The nodes of elements which belong to outer boundary are accounted for by function (11). Then the algebraic equations can be expressed by the following matrix form [15]:

$$\big\{[A] + \mu[I]\big\}\big[H_n^{i+1}\big] + [C]\big[Q_n^{i+1}\big] = \mu[F] \tag{15}$$

Here, $[A]$ and $[C]$ are the square matrices of coefficients and they are respectively relative to those coefficients of the second item and the third item of (14). $[I]$ is unit matrix which corresponds to the first item of (14). $[F]$ is the column matrix which is called load matrix corresponding to H_{n-1}. Obviously, the matrices $[A]$ and $[C]$ are dependent upon the effective conductivity σ_{sc}.

2.4 Numerical Procedures

Here we introduce the main steps of the numerical code as follows.

Step 1: Initiate the values of (15) with (13). Initial value of σ_{sc} is assumed sufficiently large at the first step of iteration.

Step 2: $t = t + dt$, $n = t$, $i = 1$.

Step 3: calculate the stiffness matrices of $[A]$, $[C]$, resolve the solution of column matrix $[H^{i+1}]$.

Step 4: calculate σ_{sc}^{i+1} by the equation: $\sigma_{sc} = J_{sc}/E_{sc}$, judge the concentration of iteration by:

$$\left|\sigma_{sc}^{i+1} - \sigma_{sc}^{i}\right| \leq \delta \tag{16}$$

where δ is a given value which used to control the precision of iteration. If all the bulk HTSC mesh nodes do not satisfy (16), then $[H^i] = [H^{i+1}]$, $i = i + 1$, and go to Step 3.

Step 5: if $n < T$, then go to Step 2. T is the upper limit of time.

After the magnetic fields and current density distribution are resolved, the magnetic forces acting on the bulk HTSC can be calculated by:

$$F_{\text{em}} = \int_v J \times B_{\text{ex}}\, dv \tag{17}$$

where V represents the volume of the bulk HTSC, J is the induced current density and B_{ex} is the external magnetic field.

The numerical integral methods are used in cell element stiffness matrices and F_{em}, i.e. (17), calculation with isoperimetric element transformation technology; it is possible to resolve any problem of non-regular geometric shape of bulk HTSC.

3 Simulation and Measurement Results and Discussion

We used the proposed methods in Sect. 2 to simulate the simple levitation system composed of a cylindrical bulk HTSC and a PMG. This levitation system is the prototype of the first man-loading Maglev system [4]. Figure 2 shows the schematic diagram of the levitation system of the simulation and experiment. The gap from positions A and B to the top surface of the PMG is 53 mm and 3 mm, respectively. Positions A and B are at the right center above the PMG. The axis line of the cylinder YBCO bulk parallels to y-direction.

The cylindrical bulk YBCO is 30 mm in diameter and 15 mm in thickness. The PMG is made of NdFeBs of 40 mm in width, 40 mm in height and 80 in length and iron yokes.

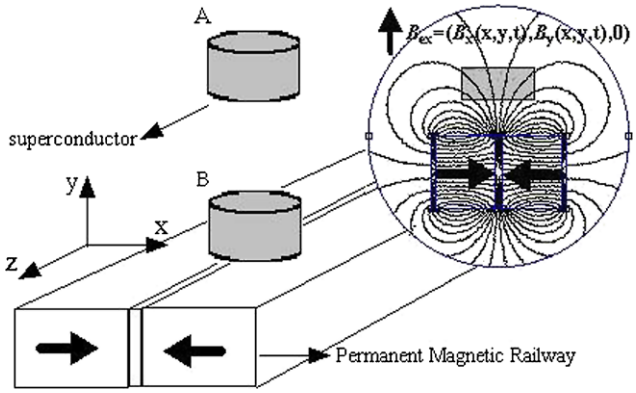

Fig. 2 YBCO bulk vs. PMG levitation system

The cross section paralleling to x-y plane of the PMG is 90 mm in width and 40 mm in height. The magnetic field induced by the PMG is symmetric in x-y plane. The up-right diagram of Fig. 2 shows it. The standard analysis method with the equivalent surface current model is used to calculate the magnetic field of PMG. Figure 3 shows the calculated and measured results of magnetic flux density with the gap from 1 mm to 55 mm at the right center above the PMG along vertical track. Figure 3 shows that the calculated values of magnetic flux density generated by the PMG are a little smaller than the measured values when the gap is low: 20 mm. When the gap decreases to less than 3 mm, the calculated value is smaller than the measured value. This is because the calculation of magnetic field of the PMG is carried out in a perfect state which ignores the influence of magnetic field concentration effect of the iron yokes. With the gap equal to 3 mm, the calculated value and the measured value of magnetic flux density of the PMG are 0.45 T and 0.47 T, respectively.

As Fig. 2 shows, during the simulation, the bulk HTSC is in zero-field-cooling (ZFC). Simple magnetic force displacement loops are simulated by this way: firstly, the sample is vertically brought down from the position A of gap equal to 53 mm to position B of gap equal to 3 mm at the right center surface above the PMG with velocity equal to 1 mm/s. After the sample gets to position B, it is brought away back to position A with the same velocity. Because the velocity is small, the displacement current is ignored.

Similar experiment instruments and progress are made to measure the levitation force between the bulk YBCO and the PMG, as Fig. 2 shows. It is a cylinder shape bulk YBCO with the diameter of 30 mm and the height of 15 mm. The bulk YBCO was made in the year 2001. In the experiment the sample is cooled by liquate nitrogen (77 K) in the case of ZFC.

For simulation, when the magnetic field solutions of the bulk HTSC are obtained, the current density distribution can be resolved by (1) mathematically. We can calculate the electromagnetic levitation force by formula (17). Figure 4

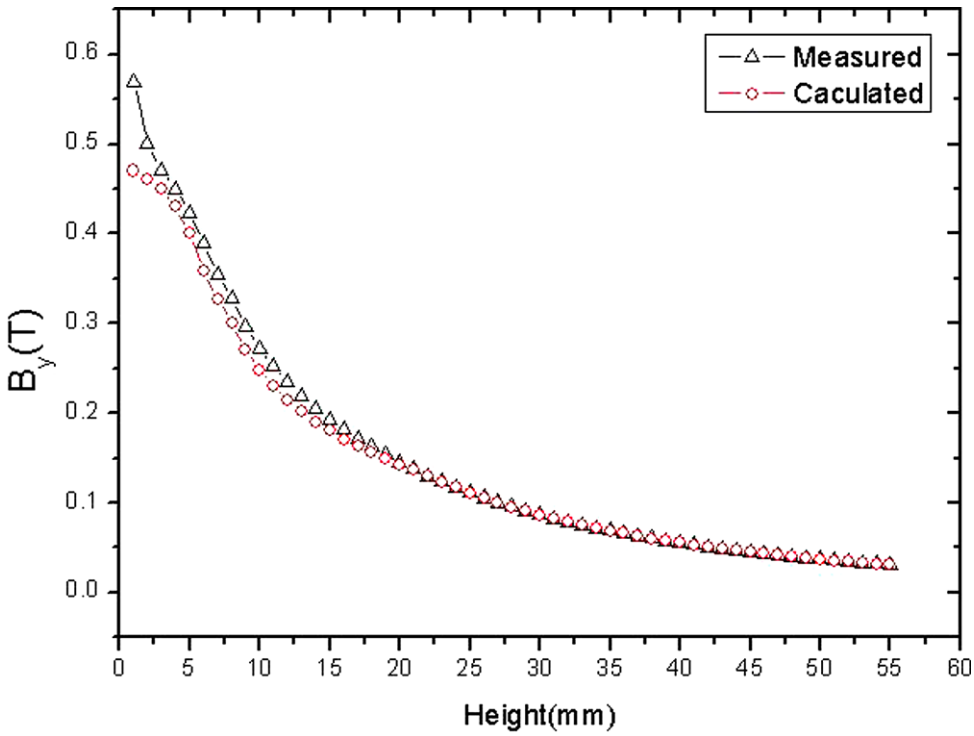

Fig. 3 Distribution of calculated and measured magnetic field of PMG of a track along the vertical direction

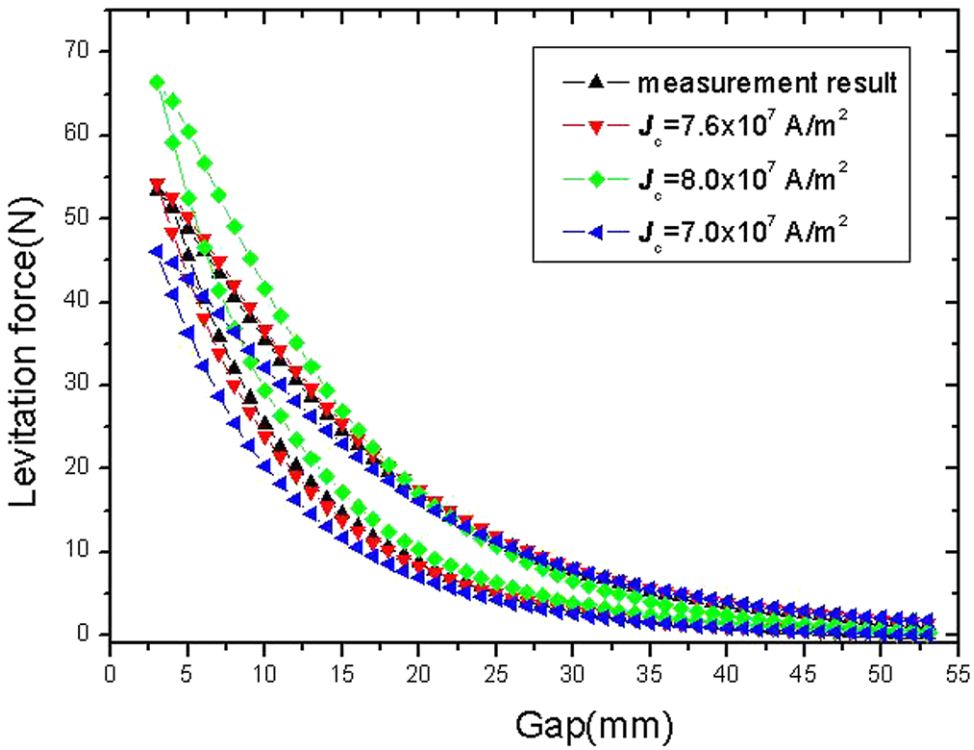

Fig. 4 Experiment and calculation of force–displacement loops plot. The minimum gap =3 mm. ($E_0 = 1.0 \times 10^{-4}$ A/m, gap = 3 mm)

shows the calculation and measurement of electromagnetic levitation forces acting on the samples.

The vertical force–displacement loops exhibit some hysteresis. This could be explained by the characteristic of HTSC magnetic hysteretic effects. When the bulk is brought vertically down to the top surface of the PMG and is brought away, hysteretic loop areas of measurement and calculation forces are different from each other. Figure 4 shows that, for calculation forces, the hysteretic loop area decreases with increasing of critical current density J_c. Generally, the mag-

netic field easily penetrates into the bulk HTSC with the low critical current density. The figure also shows that the calculation force of $J_c = 7.6 \times 10^7$ A/m^2 matches the measured force very much in hysteretic loop area and in maximum value. The value of J_c seems to be low. This may happen for two reasons. The sample was bought in 2001 and the performance of the materials was not good at that time. Almost seven years' time made the performance of the sample not good either.

4 Conclusion

A numerical method has been proposed for 3D-model high-T_c superconductor electromagnetic behavior analysis using critical model to describe the E-J characteristics of HTSC. The high-T_c superconductor nonlinear material is considered by two virtual bulk HTSC. The resolve code is successfully developed with FORTRAN language. A simple cylinder shape bulk HTSC vs. PMG levitation system is successfully simulated by the proposed method. A similar experiment of the simulation is carried out and the measured results show that the calculated and measured values match well. The presented method could be used for the HTSC Maglev transportation system optimizing design.

Acknowledgements This work is supported by the National High Technology Research and Development Program of China (863 Program: 2007AA03Z210) and Chinese National Natural Science Foundation (50777053).

References

1. Hull, J.R.: Rep. Prog. Phys. **66**, 1865–1886 (2003)
2. Murakami, M.: Physica C **341–348**, 2281–2284 (2000)
3. Moon, F.C.: Superconducting Levitation. Wiley, New York (1994)
4. Wang, J., Wang, S.: Physica C **378–381P1**, 809–814 (2002)
5. Brandt, E.H.: Phys. Rev. B **54**, 4246–4264 (1996)
6. Prigozhin, L.: J. Comput. Phys. **129**, 190–200 (1996)
7. Qin, M.J., Li, G., Liu, H.K., Dou, S.X., Brandt, E.H.: Phys. Rev. B **66**, 024516 (2002)
8. Barnes, G., McCulloch, M., Dew-Hughes, D.: Supercond. Sci. Technol. **12**, 518–522 (1999)
9. Ruiz-Alonso, D., Coombs, T., Campbell, A.M.: Supercond. Sci. Technol. **17**, s305–s310 (2004)
10. Nibbio, N., Stavrev, S., Dutoit, B.: IEEE Trans. Appl. Supercond. **11**, 2631–2634 (2001)
11. Hong, Z., Jiang, Q., Pei, R., Campbell, A.M., Coombs, T.A.: Sci. Technol. **20**, 331–337 (2007)
12. Amemiya, N., Miyamoto, K., Banno, N., Tsukamoto, O.: IEEE Trans. Appl. Supercond. **7**, 2110–2113 (1997)
13. Pecher, R., McCulloch, M.D., Chapman, S.J., Prigozhin, L., Elliott, C.M.: Paper presented at EUCAS 2003, Sorrento (2003)
14. Gou, X.F., Zheng, X.J., Zhou, Y.H.: IEEE Trans. Appl. Supercond. **17**(3), September (2007)
15. Amemiya, N., Murasawa, S.-I., Nanno, N., Miyamoto, K.: Physica C **310**, 16–29 (1998)